

On FPL configurations with four sets of nested arches

P. Di Francesco and J.-B. Zuber

*Service de Physique Théorique de Saclay,
CEA/DSM/SPhT, URA 2306 du CNRS,
F-91191 Gif sur Yvette Cedex, France*

The problem of counting the number of Fully Packed Loop (FPL) configurations with four sets of a, b, c, d nested arches is addressed. It is shown that it may be expressed as the problem of enumeration of tilings of a domain of the triangular lattice with a conic singularity. After reexpression in terms of non-intersecting lines, the Lindström-Gessel-Viennot theorem leads to a formula as a sum of determinants. This is made quite explicit when $\min(a, b, c, d) = 1$ or 2 . We also find a compact determinant formula which generates the numbers of configurations with $b = d$.

AMS Subject Classification (2000): Primary 05A19; Secondary 52C20, 82B20

Given a square grid of side n , Fully Packed Loops (FPL) are sets of paths which visit once and only once each of the n^2 sites of the grid and exit through every second of the $4n$ external edges. FPL of a given size fall into connectivity classes, or *link patterns*, of configurations with a definite set of connectivities between their external edges. The problem of enumerating FPL of a given link pattern is a challenging problem for the combinatorialist, related to alternating sign matrices and other problems of current interest (see [1,2] for reviews). It is also of relevance in statistical mechanics, as it is related by the Razumov-Stroganov conjecture [3] to the $O(1)$ -loop model of percolation, see [4] for references.

This paper, which is a continuation of [5], is devoted to a study of FPL configurations with four sets of nested arches. We shall assume the reader to have some familiarity with the ideas and techniques developed in [5] for the case of three sets of nested arches. In particular, with the notion that the boundary conditions force a certain number of edges to be occupied or empty (“fixed edges”), see also [2] for a precursor of this idea and [6] for a recent application to other types of FPL configurations.

Our aim is not only to get formulas as explicit as possible for the numbers of these FPL configurations, but also –and mainly– to see to what extent this problem is equivalent to the counting of tilings of certain domains of the triangular lattice, or in a dual picture, to that of dimer configurations on a certain graph.

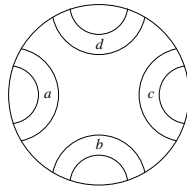


Fig. 1: The link pattern of FPL configurations with four sets of nested arches.

We shall consider FPL configurations with four sets of a , b , c and d nested arches and denote $A_n(a, b, c, d)$ their number, $n = a + b + c + d$ being the total number of arches, see Fig. 1. We recall Wieland’s theorem [7], which asserts that $A_n(a, b, c, d)$ depends only on the orbit of the FPL link pattern under the action of the dihedral group D_{2n} . Contrary to the simple case of 3 sets of arches [5], but like in the more complicated case treated in [6], we use this theorem to pick a particularly suitable representative of the orbit.

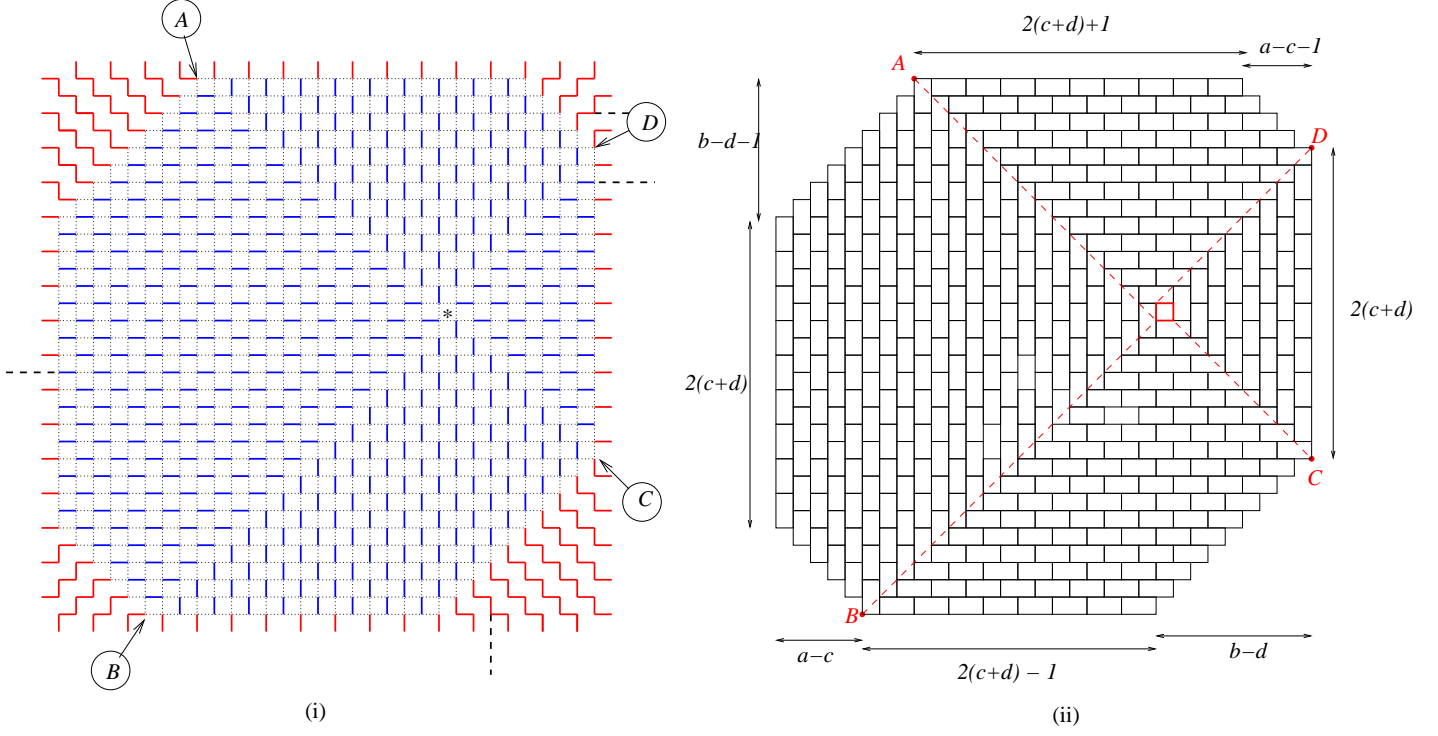


Fig. 2: The generic situation where $a > c$, $b > d$. (Here $a = 13$, $b = 10$, $c = 8$ and $d = 1$). (i) the fixed occupied edges in red or blue, the unfixed ones in dotted lines; (ii) the octagonal domino grid \mathcal{O} .

1. From FPL to dimers to non intersecting lines

1.1. The octagonal domain of unfixed edges

Using the reflective and cyclic symmetries of the problem, $A_n(a, b, c, d) = A_n(a, d, c, b) = A_n(b, c, d, a)$, we may always assume that $a \geq c$ and $b \geq d$. Let A, B, C, D denote the centers of the sets of nested arches, we assume they are in anticlockwise order. Because $2(a + b) \geq n$, A and B belong to different sides of the square. Then one uses the same procedure as in [2,5] to fix edges in 45° -cones of vertices A, B, C, D : outside these cones the occupied edges either form staircases (red edges on Fig.2 (i)), or every second (blue) edge parallel to the external ones is occupied: we refer the reader to [5] for a discussion of the procedure. The unfixed edges then live either on the sides of rectangular 2×1 tiles, also called dominos, the inner sides of which are occupied, or inside a connected domain made of adjacent elementary squares. Because the latter squares appear as defects (“disclinations” in the language of cristallography) in the tiling reinterpretation of the FPL, we try to make this domain as small as possible. The choice of a Wieland rotation which brings the diagonal lines emanating from A and C and those from B and D almost colinear, see Fig.

2 (ii), reduces this defect zone to a single elementary square (indicated by a star in Fig. 2 (i) and drawn in red in Fig. 2 (ii)). Thus

Proposition 1. *If one chooses Wieland’s rotation such that the centers of arches are as depicted in Fig. 2, every site of the lattice belongs to at least one fixed edge, and the unfixed edges form an octagonal pattern \mathcal{O} made of dominos surrounding a single elementary square.*

The locations of the points A, B, C, D and of the small square are determined by the data given in Fig. 2. We refer to this pattern of unfixed edges as the *domino grid* \mathcal{O} , to the sites which belong to a single fixed edge as *active*, and to the elementary square as the *central square*.

The figure depicts the generic situation when both differences $a - c$ and $b - d$ are greater than 0. This includes the cases where one or/and the other equals 1, and where the octagon loses some side(s) and acquires right angles.

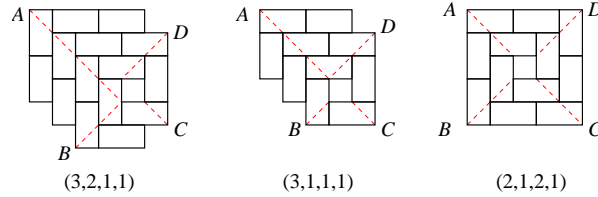


Fig. 3: Limiting cases where $a - c$ and/or $b - d$ equals 0 or 1.

In the case $a - c = 0, b - d > 0$ (or vice versa), the side of length $a - c - 1$ shrinks to naught, while the adjacent sides are reduced by one unit, hence have lengths $2(c + d) - 1$ and $2(c + d)$. One is left with a hexagonal domain with two right angles, see Fig. 3. If both $a = c$ and $b = d$, one gets a rectangle.

Given this set of fixed edges, an FPL configuration is determined by an appropriate choice of *dimers*, i.e., of pairings, between the active sites, realizing the desired connectivity pattern. In particular, there are two special configurations, that we call the “empty” and the “full” ones. These configurations are obtained by dividing the domain \mathcal{O} into subdomains and choosing the dimers as indicated in Fig. 4.

Thus to any FPL configuration corresponds a dimer configuration. This correspondence between the set of FPL configurations of type (a, b, c, d) and the set of dimer configurations on \mathcal{O} cannot, however, be one-to-one. Indeed it is clear from our discussion that the domino grid is common to all FPL types $(a + p, b - p, c + p, d - p)$ for all $p, -c \leq p \leq d$.

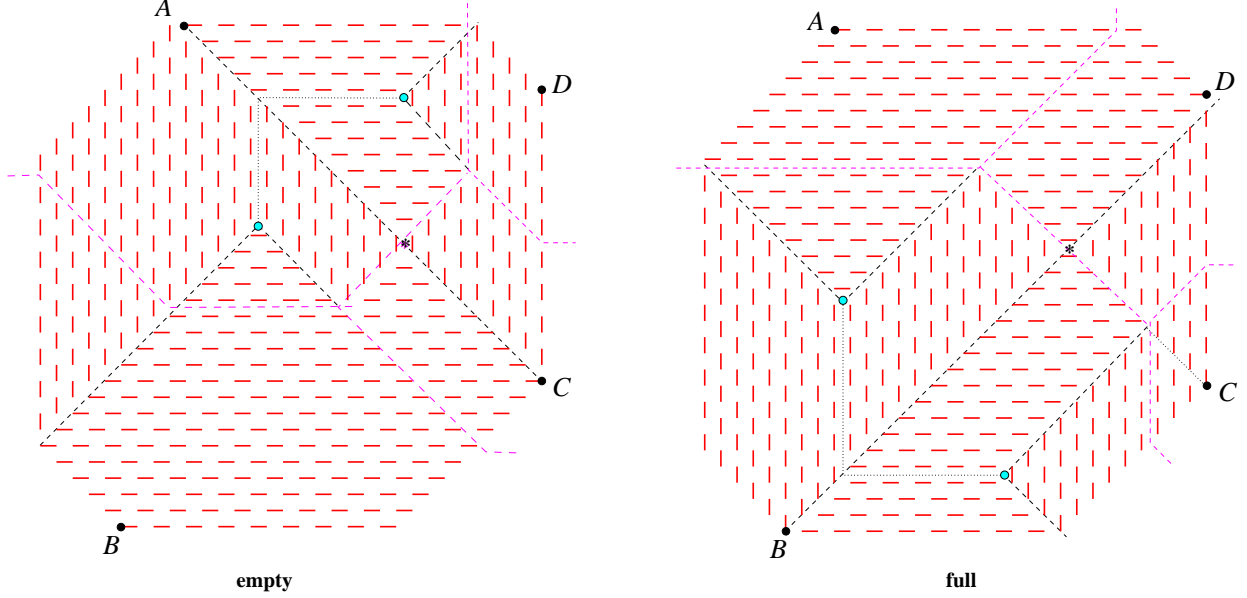


Fig. 4: The dimers of the empty and the full configurations, for $(a, b, c, d) = (9, 14, 4, 5)$. The broken black lines show how to define the limits of the various domains, while the pink ones give the limits of the sets of nested arches. The light blue dots will be explained below in sect. 1.4.3.

This is obvious in Fig. 2 where the effect of $(a, b, c, d) \rightarrow (a \pm 1, b \mp 1, c \pm 1, d \mp 1)$ is just to shift the boundaries between the different sets of nested arches (the broken black lines in Fig.2 (i)), while preserving the points A, B, C, D , the shape of the octagon, the domino grid and the location of the central square.

To distinguish dimer configurations pertaining to different p 's, we now introduce a new feature, made of non intersecting lines.

1.2. Tilings and de Bruijn lines

At this stage we find it useful to introduce the dual picture, where one constructs a triangle around each active site. The central square is also triangulated by four triangles. One gets an octagonal picture \mathcal{O}' which is depicted in Fig. 5, in (i) for the simple FPL $(2, 1, 1, 1)$ and in (ii) for a more generic one.

A final transformation consists in cutting this octagon along a line L starting from the central square, deforming the grid into a domain \mathcal{D} of the regular triangular lattice and identifying the two sides L_{\pm} of the cut. Figure 5 (iii) shows one particular way to do this. For future use, we also draw a segment L' which joins the center of the central square to the “East-North-East” corner of the octagon. (Note that the segments L and L' do not coincide with the lines used in the construction of Fig. 2, although they are parallel and

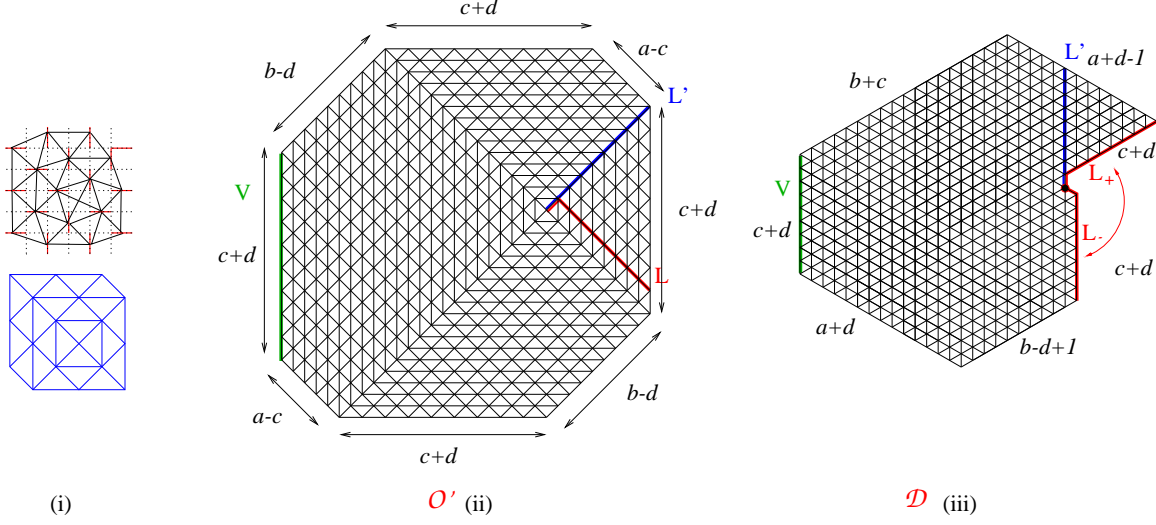


Fig. 5: Triangulating the octagonal grid. Here (i) $a = 2, b = c = d = 1$ and (ii), (iii) $a = 9, b = 14, c = 4, d = 5$.

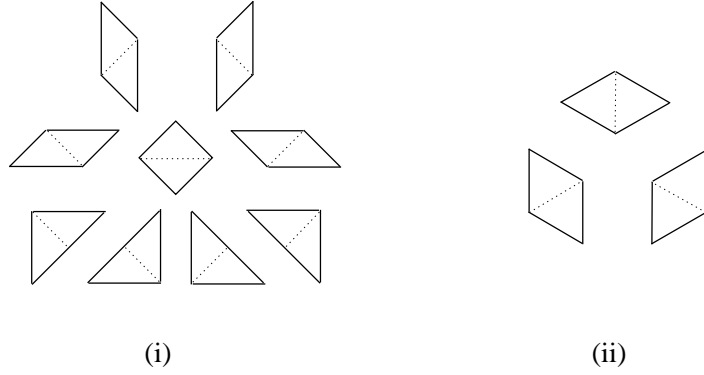


Fig. 6: The different types of tiles: (i) on the octagonal grid, (ii) after its deformation to equilateral triangles.

close to them. Below, we shall slightly modify them, in a way depending on the tiling at hand, so as to prevent them from intersecting the tiles.)

Any FPL configuration yields a pairing between triangles sharing an edge, hence a tiling of the octagon by means of the tiles depicted in Fig. 6. Just as in the previous section, the tilings of the domain \mathcal{D} comprise all cases $(a + p, b - p, c + p, d - p)$, for p running from $-c$ to d .

For a particular (a, b, c, d) , we have to find a refined characterization of the tiling configurations. We do this by means of an alternative representation by systems of non intersecting lines, also known as de Bruijn curves [8,9].

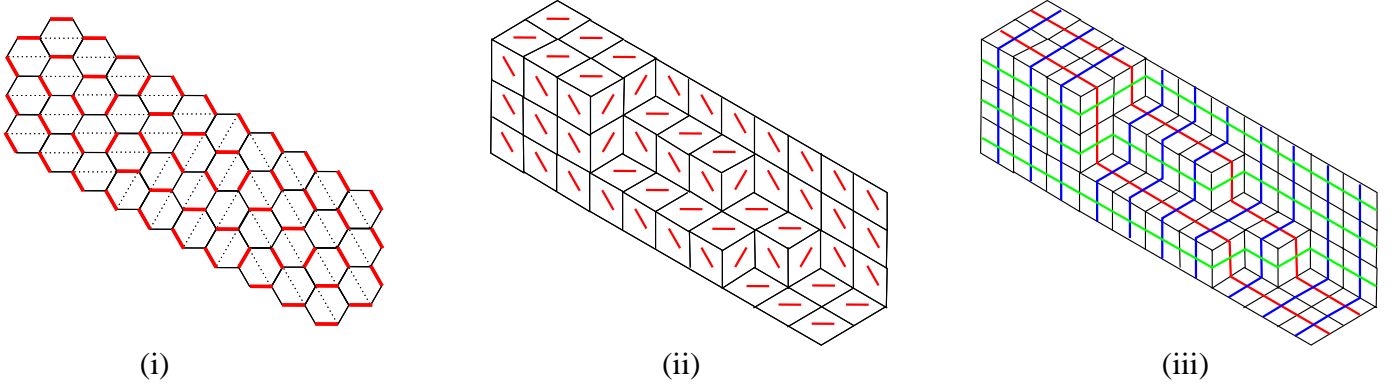


Fig. 7: The alternative descriptions of a plane partition, (i) as a set of dimers on the honeycomb lattice, (ii) as a tiling or stack of cubes, and (iii) as a system of non-intersecting lines of either of three colours.

Recall that in the simple case of the tiling of a hexagon of size $a \times b \times c$, or equivalently of the plane partitions in a box of that size, there is a one-to-one correspondence between (i) configurations of dimers on a domain of the honeycomb lattice, (ii) configurations of tiles (in the tiling problem of the hexagon) or of elementary cubes (in the plane partition picture), and (iii) any of the three families of non intersecting lines joining a pair of opposite sides of the hexagon, see Fig. 7. Each family describes a collection of strips of tiles, which pairwise share edges parallel to a given direction.

1.3. The **c** and **d** lines: definition and properties

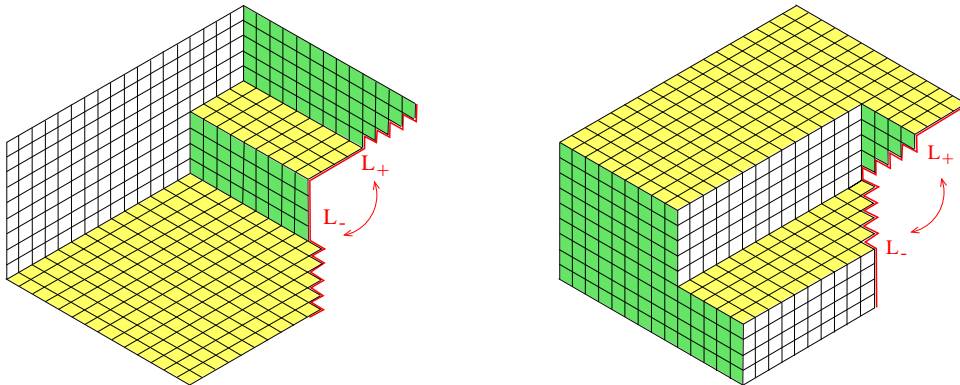


Fig. 8: Tiling of the empty and full configurations.

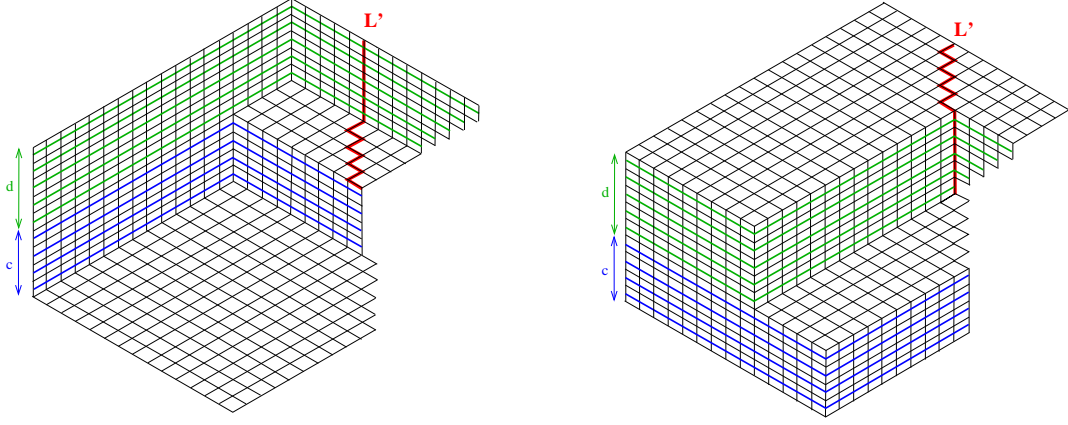


Fig. 9: The de Bruijn lines of the empty and full configurations. The segment L' appears in red, slightly deformed so as to follow tile edges.

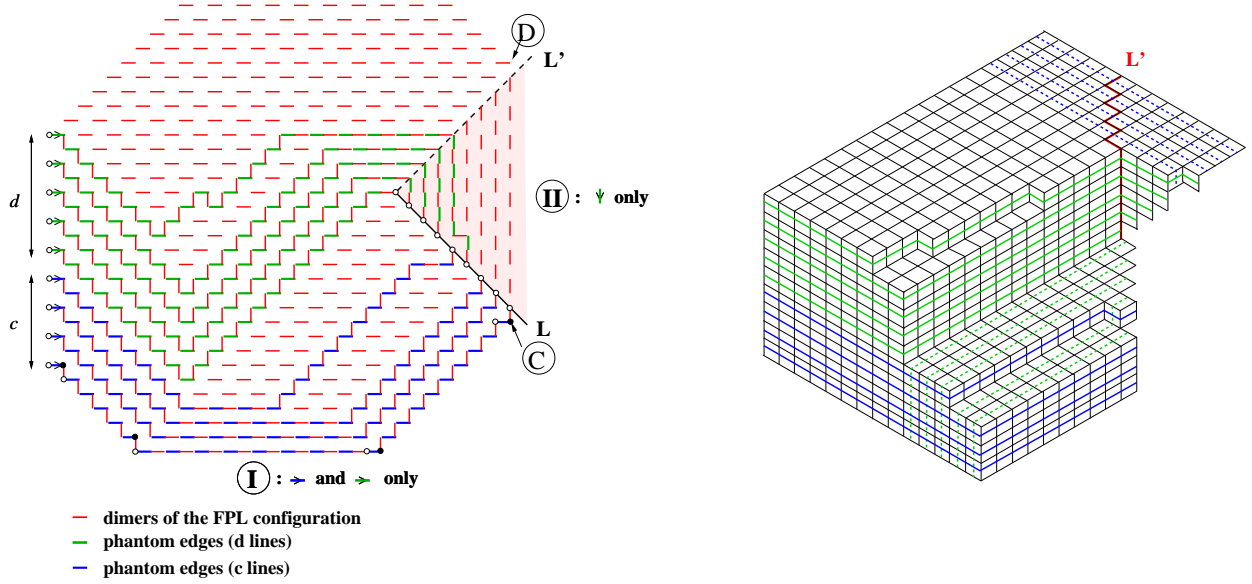


Fig. 10: The c (blue) and d (green) lines of a FPL configuration of type $(9, 14, 4, 5)$. On the right figure, they have been continued across the cut as broken lines.

Given the tiling associated with a certain FPL configuration of type (a, b, c, d) , consider the $c + d$ de Bruijn lines which start from the vertical left side V of the domain \mathcal{O}' of Fig. 5 (ii) or \mathcal{D} of Fig. 5 (iii). As noticed above, the tiling is made of strips of tiles, pairwise sharing edges parallel to a given direction, and the de Bruijn lines join the middles of these edges: see for example the tilings and these lines for the empty and full configurations in Fig. 8 and 9. These lines are non-intersecting, and we call c lines the first c starting from the bottom of the left vertical interval V , and d lines, those (in number d) which start from the upper part of that interval. We continue these lines across the domain until they

reach the line L or exit through the boundary of \mathcal{O}' , whichever occurs first. In fact, we claim (and will prove below) that they all reach the line L first, and more precisely, that the \mathbf{c} lines will reach it from below, while the \mathbf{d} ones will do it from above. On the domain \mathcal{D} , the \mathbf{c} lines reach the lower cut L_- while the \mathbf{d} lines reach the upper one L_+ . We now state the main result of this paper:

Theorem 1. *There is a bijection between FPL configurations of type (a, b, c, d) and families of \mathbf{c} and \mathbf{d} non intersecting lines on \mathcal{D} , where the \mathbf{c} lines go from V to L_- , and the \mathbf{d} lines go from V to L_+ . The sets of points where the \mathbf{c} lines and the \mathbf{d} lines reach L are disjoint.*

This theorem has been stated for the lines on \mathcal{D} but can of course be rephrased on \mathcal{O}' . Because the endpoints on L of the \mathbf{d} lines are disjoint from those of the \mathbf{c} , we allow a slight (configuration-dependent) redefinition of the lines L_{\pm} on the domain \mathcal{D} so as to make them lie along tile edges, see Fig. 8.

To prove this theorem, we establish a certain number of properties of the \mathbf{c} and \mathbf{d} lines, going back and forth between the two pictures, on the octagonal grid \mathcal{O} on the one hand, on the cut domain \mathcal{D} one on the other. The properties of the lines are indeed easier to establish in the tiling version, but to discuss their interplay with the FPL paths, it is essential to return to \mathcal{O} .

The first step is thus to translate the construction of the \mathbf{c} and \mathbf{d} lines back to the octagonal grid \mathcal{O} . By a slight abuse of notation, we still denote them by \mathbf{c} , \mathbf{d} on \mathcal{O} . Note that the (active) sites of \mathcal{O} are bicolorable. By convention, we assign the color \bullet to point C and to all sites distant from it by an even number of lattice steps, and \circ to the others. (For the sake of clarity, only a few sites have been colored in Fig. 10.) When drawn on \mathcal{O} , the two segments L and L' start from the upper right corner of the central square and pass by the external endpoints of the two empty edges entering the FPL grid at the points C and D , respectively ¹. These lines divide the octagonal domain \mathcal{O} into two regions I and II, see Fig. 10. Note that, by the construction of the subsection 1.1, region II contains all the horizontal fixed edges of the right part of \mathcal{O} and segments L and L' pass through their leftmost endpoints. Now, for a given FPL configuration of type (a, b, c, d) , associated with a certain choice of dimers on the domino grid \mathcal{O} , we call *vacant* the yet unused edges of \mathcal{O} .

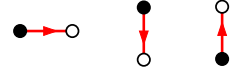
¹ This last assertion has to be slightly amended in the case where $a = c, b = d$ and the four points A, B, C, D lie at the corners of the octagon, which has degenerated into a square (see Fig. 3).

The **c** and **d** lines start from the $c + d$ vacant horizontal external edges bordering the left vertical side of the domino grid and are oriented inwards the grid. They visit alternately a vacant edge and a dimer of the FPL configuration, with the rule that the chosen vacant edges (called *phantom*) are all horizontal (and oriented from left to right) in region I and vertical (and oriented from top to bottom) in region II. This rule is just the transcription of the definition of the **c** and **d** lines on \mathcal{D} , namely it reflects the pairing of adjacent tiles which share a vertical edge.

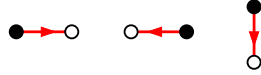
In the same way as on \mathcal{D} , the first c lines from the bottom are called **c** lines, the next d are called **d** lines, and we interrupt them as soon as they touch either the segment L or one of the boundaries of the grid. Note that the fact that the lines may be constructed without encountering any obstruction or that they are non-intersecting, which is not obvious from the standpoint of \mathcal{O} , follows from their construction on the domain \mathcal{D} as conventional de Bruijn lines. This is summarized in

Lemma 1. *On \mathcal{O} , the **c** and **d** lines are non intersecting; each of them is described by an alternate sequence of dimers and of “phantom” edges.*

*In region I the dimers visited by the **c** and **d** lines are of the three types*



while in region II, they are:



Another property of **c** and **d** lines which is clear from their definition on \mathcal{D} is the fact that between two of them, or below the lowest one, or above the highest one, the tiling is frozen and uses only horizontal rhombi. This is easily established, starting from the leftmost corner of any domain of the triangular lattice lying between two successive lines, or between the upper or lower one and the boundary, and proceeding iteratively. This also means that the data of **c** and **d** lines are sufficient to characterize the tiling entirely. When restated on \mathcal{O} , this property means that **c** and **d** lines are separated in region I by only horizontal dimers and in region II by only vertical ones. Moreover, these separating dimers connect \circ sites to \bullet ones from left to right in region I and from top to bottom in region II. We thus have

Lemma 2. *All vertical dimers of the region I and all horizontal dimers of region II are visited by **c** or **d** lines. Also, all horizontal dimers connecting \bullet to \circ sites from left to right in region I and from top to bottom in region II are visited by **c** or **d** lines.*

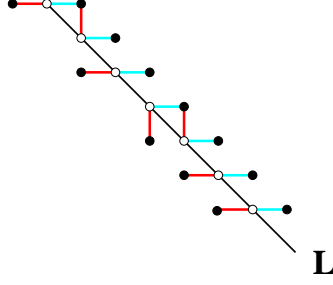


Fig. 11: The immediate neighborhood of L . Dimers are represented in red, and fixed edges in light blue. Only two situations may occur for FPL paths: either they cross L via a dimer on the left and a fixed horizontal edge on the right, or they simply touch L without crossing via a fixed edge followed by a dimer on the right side.

Lemma 3. *All c and d lines must go to L .*

This is obvious on \mathcal{D} : the c and d lines enter \mathcal{D} through vertical edges along V ; they must necessarily exit through vertical edges again, and the only possibility to do so is through L_{\pm} , see Fig. 10. From the standpoint of \mathcal{O} , this is less obvious: by parity arguments, all sites of \mathcal{O} on L are \circ sites. By lemma 2, it follows that any c or d line reaching L must do so via a dimer. On Fig. 2 we observe that no fixed edge may touch L from the left side hence the only way a FPL path may touch L from the left is via a dimer, which, as it ends up on a \circ site, must by Lemma 2 be also part of a c or d line. So any FPL path that touches L from the left and therefore crosses it, as it is prolonged via a fixed horizontal edge on the right of L , corresponds to the end of a c or d line coming from the left. Analogously, any FPL path touching L from the right but not crossing it corresponds to the end of a c or d line coming from above. By fully-packedness, only these two situations (crossing, or touching from the right without crossing) may occur, in view of the disposition of fixed edges, see Fig. 11 for illustration. On the total of $c + d$ sites of L , some of them, say i , correspond to crossings of FPL paths, and the other $c + d - i$ to touching without crossing. These add up to the $c + d$ c and d lines introduced above.

Lemma 4. *$i = c$, hence all c lines reach L from the left and all d lines reach it from above.*

As noted above, the external endpoint of L is the center of the set of c FPL nested arches. It is clear that these arches must cross either L or its prolongation across the central square. Let us show that they cross L and that they are in one-to one correspondence with the c or d lines ending up on L from the left. Let us prolongate the lines crossing L into FPL paths by letting them alternate between fixed edges and dimers. The fixed edges on the right of L being all horizontal, let us orient them from left to right. The FPL paths visit them in

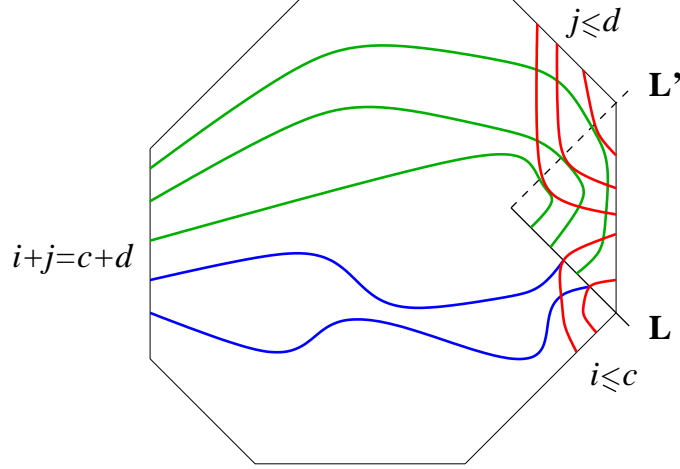


Fig. 12: Each of the i **c** or **d** lines terminating on L from the left corresponds to an FPL arch centered on C , hence $i \leq c$. The same holds for the j **c** or **d** lines touching L' from the left: each of them correspond to a FPL arch centered on D , hence $j \leq d$. But as $i + j = c + d$, we must have $i = c$ and $j = d$

this direction. In particular, such a path can never cross L again and can only bounce off it. This means that all FPL paths crossing L must exit \mathcal{O} along its right border. The same reasoning in the region to the left of L shows that these FPL paths must enter the grid from the lower border. The c FPL paths are the only ones which connect the bottom to the right, and therefore $i \leq c$, see Fig.12. The same reasoning applied to the line L' , with c replaced by d shows that there are $j \leq d$ **c** or **d** lines crossing L' . But the only way for a **c** or **d** line to reach L from above is by first crossing L' , hence there are at most $j \leq d$ **c** or **d** lines reaching L from above. As the total of **c** and **d** lines reaching L is $c + d = i + j$, we must have $i = c$ and $j = d$.

Lemma 5. *From the non-intersecting **c** and **d** lines, one reconstructs a unique FPL configuration of type (a, b, c, d) .*

We start from a configuration of non-intersecting **c** and **d** lines going from the left vertical border V of \mathcal{O} to the line L , with the rule that every second edge is horizontal and travelled from left to right in region I and vertical and travelled from top to bottom in region II, while the arrival sites on L form two disjoint sets of respectively c and d sites. We then construct dimers by keeping every second edge (those going from a \bullet to a \circ) on the **c** and **d** lines, and adjoining them the horizontal edges connecting \circ to \bullet sites from left to right in region I, and from top to bottom in region II, in all regions between the **c** and/or **d** lines: this gives a complete dimer covering. Upon addition of the fixed edges as specified in sect. 1.1, one gets a FPL configuration. By the same argument as in Lemma 4, there

are c FPL paths crossing L and d crossing L' . This exhausts all external edges on the right vertical side of the grid, and therefore the sets of c and d nested arches are next to one another.

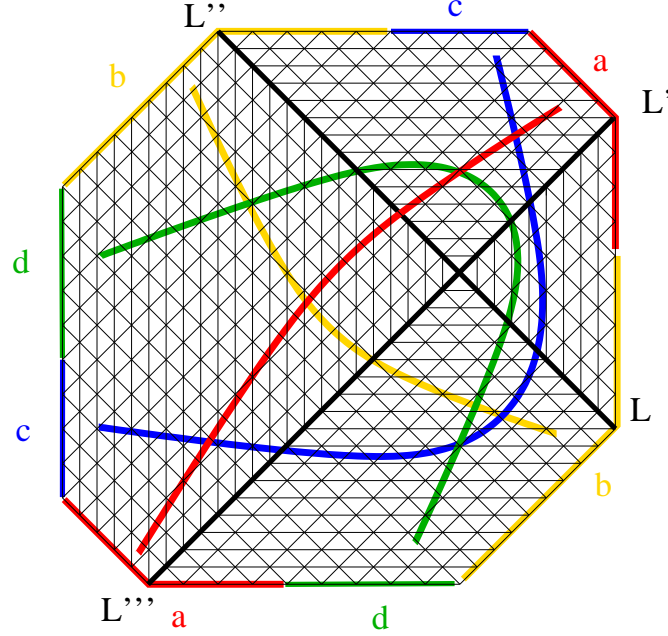


Fig. 13: Artist's view of the **a**, **b**, **c**, **d** lines on \mathcal{O}' .

The same discussion must now be repeated for the pairs (d, a) and (b, c) . One introduces the two new sets of lines **a** and **b**, which start from the segments of the boundary of \mathcal{O}' marked in Fig. 13, and which are de Bruijn lines describing chains of tiles sharing edges parallel to a certain direction. One also continues the previous lines **c** and **d** across the segment L up to the boundary. The segments L'' and L''' , which are the continuations of L and L' , respectively, across the center of the central square, have lengths $a + d$ and $b + c$. One may then apply the analysis of Lemmas 1-5 to the pairs (\mathbf{a}, \mathbf{d}) and (\mathbf{b}, \mathbf{c}) . In particular, there are a FPL paths centered on A which cross the segment L'' on sites disjoint from those of the **d** lines; and likewise for the **b** lines centered on B and the **c** lines, across the segment L''' . One concludes that the FPL configuration contains at least four sets of a , b , c and d nested arches. As $a + b + c + d = n$, this exhausts the number of FPL paths (and possibly also the patience of the reader!), establishes the Lemma and completes the proof the Theorem.

1.4. Remarks

1. From the discussion above, in particular from Lemma 5, it follows that






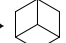
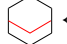
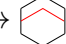
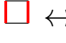
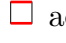
Corollary *Any dimer configuration on the octagonal grid \mathcal{O} or any tiling of \mathcal{O}' yields a FPL of type $(a + p, b - p, c + p, d - p)$, for some p , $-c \leq p \leq d$.*

Indeed, start from the domino grid pertaining to any (a, b, c, d) FPL configuration. For any dimer configuration on \mathcal{O} or the associated tiling of \mathcal{O}' , draw the corresponding non intersecting lines on \mathcal{D} . Let c' be the number of those which reach L_- , d' that of those reaching L_+ , with $c + d = c' + d'$. By lemma 5, one reconstructs a unique FPL configuration of type (a', b', c', d') with $a' - a = c' - c = b - b' = d' - d =: p$.

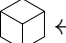
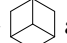
This corollary implies a sum rule on numbers of FPL configurations in terms of that of dimers

$$\sum_{p=-\inf(a,c)}^{\inf(b,d)} A_n(a + p, b - p, c + p, d - p) = \# \text{dimers on } \mathcal{O}, \quad (1.1)$$

of which we shall present examples in sect. 2.3.

2. It is legitimate to ask if the elementary moves  \leftrightarrow  or  \leftrightarrow  on dimers are ergodic, i.e. suffice to span all the FPL configurations of a given type (a, b, c, d) . Equivalently, are the moves  \leftrightarrow  acting on tilings ergodic? Contrary to the case of three sets of nested arches [5], we cannot rely on the picture of cube stacking, because of the conic singularity in the tiling caused by the cut. The third picture we used, namely the non intersecting lines, provides the answer. It is easy to prove by contradiction that all configurations of non intersecting lines \mathbf{c} and \mathbf{d} on the domain \mathcal{D} are generated from one of them by repeated applications away from the branch point of the elementary move  \leftrightarrow  (and their rotated). This establishes the ergodicity property for the above moves of dimers or of tiles ². Note on the other hand that the move  \leftrightarrow  acting on the central square connects FPL configurations of types (a, b, c, d) and $(a \pm 1, b \mp 1, c \pm 1, d \mp 1)$.

3. In view of this ergodicity, we may now reconsider the two special configurations, “empty” and “full”, depicted in Fig. 4 and 8. What makes them extremal is the fact that only *two* elementary moves can act upon them. (This should be compared with the unique move in the ordinary case of cube stacking, when one considers the empty or the full box.) The locations of these moves are what is represented by the blue dots in Fig. 4.

² This result is stronger than the classical result stating that the moves  \leftrightarrow  are ergodic on tilings of simply connected domains of the triangular lattice [10].

4. Note that the tiling problem we have to deal with is reminiscent of but not identical to the problem treated in [9], namely that of a centro-symmetric octagon by six species of tiles.

2. Counting configurations.

In this section, we use the bijection of Theorem 1 to actually count the numbers of FPL configurations of type (a, b, c, d) .

2.1. The setting

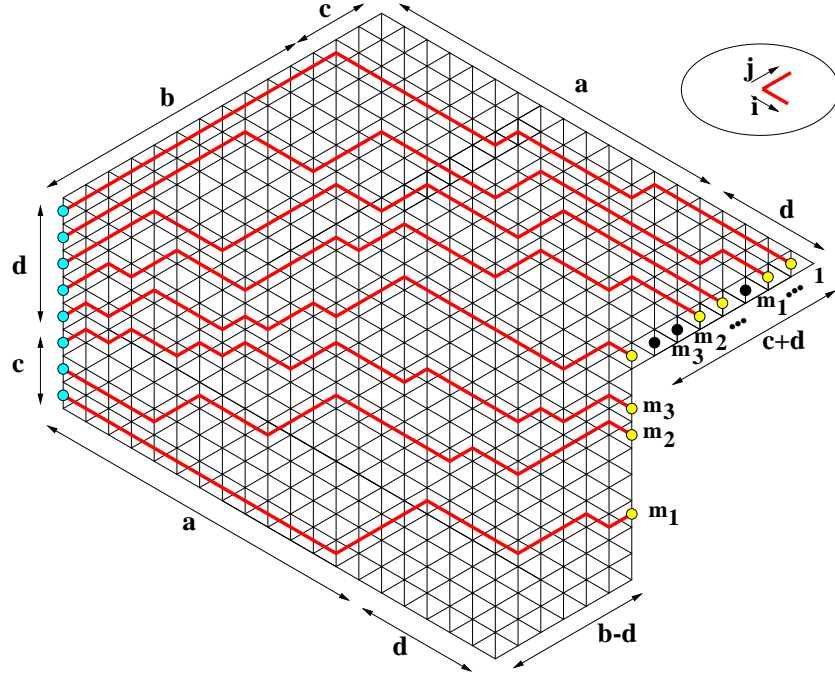


Fig. 14: A typical configuration of non-intersecting c and d lines for $c = 3$, contributing to $f_{m_1, m_2, m_3}(a, b, 3, d)$. The lines must enter through the light blue points (on the left) and exit through the upper part of the cut except at the points m_1, m_2, m_3 or through its lower part, at the points m_1, m_2, m_3 . The elementary steps for the c and d lines, in directions i and j , are shown in the medallion.

It is simplest to use the c and d lines on the domain \mathcal{D} . The fact that they stop on segments L_{\pm} reduces the counting of configurations to the standard problem of enumerating all non-intersecting paths from one set of points to another. As the tiles crossed by c and d lines only have two orientations (and all have two vertical edges), the corresponding paths may only go in two directions say i, j at each point, as shown in the medallion of Fig.14.

Moreover, we know that the **c** lines end on the lower part of the cut L_- at c distinct points, marked in yellow in Fig.14, and that the **d** lines reach the upper part of the cut L_+ on d distinct points, forming the complement of the c . Let us denote by m_1, m_2, \dots, m_c the positions of these c points counted from bottom to top on L_- , with $1 \leq m_1 < m_2 < \dots < m_c \leq c + d$, while their positions must be counted from top to bottom on L_+ .

We now have the well-posed problem of computing the number of configurations of non-intersecting **c** and **d** lines with elementary steps **i** or **j** going on \mathcal{D} from its left side (light blue points in Fig.14) to its right (yellow points in Fig.14), and such that the lower c lines exit through points m_1, m_2, \dots, m_c of the lower part of the cut, while the upper d ones exit through their d complements on the upper part of the cut. We denote by $f_{m_1, m_2, \dots, m_c}(a, b, c, d)$ the number of such configurations.

2.2. A fermionic formula for path counting

In this section we recall the so-called Lindström-Gessel-Viennot [11] formula for counting the number $N(A_1, A_2, \dots, A_N | E_1, E_2, \dots, E_N)$ of non-intersecting paths from a set of points A_1, A_2, \dots, A_N to a set of points E_1, E_2, \dots, E_N of the square lattice, such that only elementary steps to the right and to the top are allowed. Let $P(A_i, E_j)$ denote the number of paths from the point A_i to the point E_j with these only allowed elementary steps, then we have (see [11] and further references in [12])

$$N(A_1, A_2, \dots, A_N | E_1, E_2, \dots, E_N) = \det (P(A_i, E_j))_{1 \leq i, j \leq N} \quad (2.1)$$

(For physicists, recall this is just the expression of the $2N$ -point function $\langle \psi_{A_1} \dots \psi_{A_N} \psi_{E_1}^* \dots \psi_{E_N}^* \rangle$ of free fermions, expressed as the Slater determinant of their 2-point function $P(A_i, E_j) = \langle \psi_{A_i} \psi_{E_j}^* \rangle$, when their action is $\sum_{\alpha \rightarrow \beta} \psi_\alpha^* \psi_\beta$, summed over all edges $\alpha \rightarrow \beta$ of the square lattice, oriented from left to right and from bottom to top.)

2.3. Computation of $A_n(a, b, c, d)$

To apply formula (2.1) to the computation of $f_{m_1, \dots, m_c}(a, b, c, d)$, we just have to record the relative positions of the entry and exit points of the **c** and **d** lines. The solution goes as follows. We first construct the matrix \mathcal{M} of size $(c + d) \times (c + d)$ whose $\mathcal{M}_{i,j}$ entry is the binomial coefficient

$$\mathcal{M}_{i,j} = \binom{a + b + c + d - j}{a + d - i}. \quad (2.2)$$

The matrix element $\mathcal{M}_{i,j}$ counts generically the number of paths between the i -th entry point counted from bottom to top (in light blue in Fig.14) and the j -th exit, counted from top to bottom on the upper part of the cut (in yellow in Fig.14). To take into account the missing images of the points on the lower part of the cut (filled black dots in Fig.14), we must erase the columns $j = m_1, m_2, \dots, m_c$ of this matrix, and append instead c new columns v_k , $k = 1, 2, \dots, c$,

$$(v_k)_i = \binom{a+b}{a+c+2d+1-i-m_k}, \quad (2.3)$$

which count the total number of paths from the i -th entry point to the exit point m_k on the lower part of the cut. Then the determinant of the resulting matrix $\mathcal{M}(m_1, m_2, \dots, m_c)$ gives $f_{m_1, \dots, m_c}(a, b, c, d)$:

$$f_{m_1, \dots, m_c}(a, b, c, d) = \det(\mathcal{M}(m_1, m_2, \dots, m_c)) \quad (2.4)$$

and finally

$$A_n(a, b, c, d) = \sum_{1 \leq m_1 < m_2 < \dots < m_c \leq c+d} f_{m_1, m_2, \dots, m_c}(a, b, c, d) \quad (2.5)$$

This formula is very explicit if not too easy to manipulate. We have been able to drastically simplify it in a few cases. For instance, when $c = 1$, one may expand $\det \mathcal{M}(m)$ with respect to its added column, and use an explicit expression for the inverse matrix of \mathcal{M} to prove that

$$\begin{aligned} f_m(a, b, 1, d) &= \frac{\binom{b}{d+1-m} \binom{d}{m-1}}{\binom{a+2d+1-m}{a} \binom{2d+1-m}{m-1} \binom{b+d+1}{m-1}} \frac{\prod_{i=0}^d \binom{a+b+i}{a}}{\prod_{i=0}^{d-1} \binom{a+i}{a}} \times \\ &\times \sum_{j=0}^{m-1} \frac{\binom{2d+2-m}{m-1-j} \binom{2d+2+j-2m}{j} \binom{a+m-2-j}{m-1-j} \binom{b+d+2+j-m}{j}}{\binom{m-1}{j}}. \end{aligned} \quad (2.6)$$

For $c = 2$ we have

$$\begin{aligned} f_{m_1, m_2}(a, b, 2, d) &= \frac{\binom{b}{d+1-m_1} \binom{b+1}{d+2-m_2} \binom{d+1}{m_1-1} \binom{d}{m_2-2}}{\binom{a+2d+2-m_1}{a} \binom{a+2d+2-m_2}{a} \binom{b+d+3}{m_1-1} \binom{b+d+2}{m_2-2}} \frac{\prod_{i=0}^{d+1} \binom{a+b+i}{a}}{\prod_{i=0}^{d-1} \binom{a+i}{a}} \times \\ &\times \sum_{j_1=0}^{m_1-1} \sum_{j_2=0}^{\min(m_2-2, m_2-m_1+j_1)} \left(1 - \frac{\binom{j_2}{m_2-m_1}}{\binom{j_1+m_2-m_1}{m_2-m_1}} \right) \frac{(m_2-m_1)(m_2-m_1-(j_2-j_1))}{(m_2-1-j_2)(d+2-m_1)} \times \\ &\times \frac{(2d+4-m_1)(2d+3-m_1)(2d+4-m_2)(2d+3-m_2)}{(2d+5+j_1-2m_1)(2d+5+j_2-2m_2)(2d+5+j_1-m_1-m_2)(2d+5+j_2-m_1-m_2)} \times \\ &\times \binom{a-3+m_1-j_1}{a-2} \binom{a-3+m_2-j_2}{a-1} \binom{b+d+4+j_1-m_1}{j_1} \binom{b+d+4+j_2-m_2}{j_2} \end{aligned} \quad (2.7)$$

This follows from a double expansion of $\det \mathcal{M}(m_1, m_2)$ with respect to the two added columns.

Both expressions yield pretty explicit formulas for $N(a, b, 1, d)$ and $N(a, b, 2, d)$.

2.4. FPL and dimer countings

According to the third remark of sect. 1.4 and eq. (1.1), it may be interesting to compute also the total number of dimers on the octagonal grid \mathcal{O} .

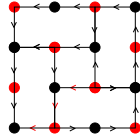


Fig. 15: Dimer counting : the case $(1,1,1,1)$.

We shall illustrate this by an example. In the cases of an $(m, 1, m, 1)$ FPL, the domino grid \mathcal{O} is made of a unit square surrounded by rectangular dominos. According to Kasteleyn [13], one computes the number of dimers on this graph by orienting its edges in such a way that along every elementary closed circuit the number of edges of either orientation is odd. The number of dimers is then the pfaffian of the resulting signed adjacency matrix. The case $m = 1$ is depicted in Fig. 15.

Since these graphs are 2-colored, their (antisymmetric) signed adjacency matrix is made of two off-diagonal blocks,

$$\begin{pmatrix} 0 & G_m \\ -G_m^T & 0 \end{pmatrix}$$

and the pfaffian is just (up to a sign) the determinant of one of these blocks. (It is 9 for the case $(1, 1, 1, 1)$).

In general, one constructs the graphs and their adjacency matrix by a recursive procedure of adding layers of dominos, as depicted in Fig. 16.

One finds that the determinants D_m , thus the numbers of dimers, are alternatingly perfect squares or doubles of perfect squares. This is a consequence of the 4-fold symmetry of the grid, as discussed in [14]. (In the terminology of that paper, the graphs G_m are 4-odd-symmetric, and their \mathbb{Z}_4 quotient has $(m + 1)^2$ vertices.)

$$d_m := \sqrt{D_{2m-1}} = 3, 70, 13167, 20048886, 247358122583, 24736951705389664, \\ 20054892679528741176540, 131821539275853806053297420440, \dots \quad \text{for } m = 1, 2, \dots, 8$$

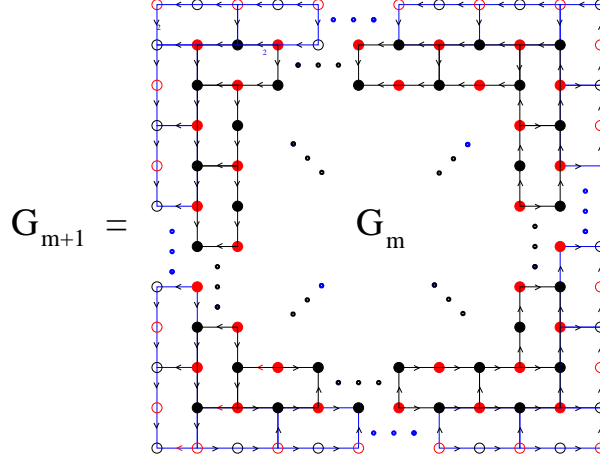


Fig. 16: Constructing G_{m+1} from G_m (in black) by adding one layer of (blue) dominos.

while

$$\begin{aligned} \delta_m &:= \sqrt{D_{2m}/2} = 8, 526, 280772, 1215446794, 42663813089328, \\ &12142696908022734304, 28022410984084414473869168, \\ &524367885668519092847372976461256, \dots \quad \text{also for } m = 1, 2, \dots, 8 \end{aligned}$$

Curiously, one observes ³ that these numbers are given by the determinant $\hat{D}(L, \theta) := e^{-i\theta L/2} \det_{1 \leq i, j \leq L} \left(\binom{i+j-2}{i-1} + e^{i\theta} \delta_{ij} \right)$ for $\theta = \pi/2$, namely that $\sqrt{D_m} = \hat{D}(m+1, \pi/2)$. This may be proved by writing $\hat{D}(m+1, \pi/2) \hat{D}(m+1, -\pi/2) = \det(I + T^2)$, where T is the matrix with entries $T_{ij} = \binom{i+j-2}{i-1}$, $i, j = 1, 2, \dots, m+1$, and expanding the determinant in terms of multiple minors of T^2 . More precisely, introducing $\Delta_m(\lambda) = \det(\lambda I + T^2)$, we have the expansion

$$\Delta_m(\lambda) = \sum_{k=0}^{m+1} \lambda^{m+1-k} \sum_{1 \leq p_1 < \dots < p_k \leq m+1} \det_{1 \leq i, j \leq k} ((T^2)_{p_i, p_j}) \quad (2.8)$$

The coefficient of λ^{m+1-k} in this polynomial is then identified with the sum of determinants (2.5), with $a = m+1-k, b = k, c = m+1-k, d = k$, by expanding the latter with respect to some of their columns as follows. Upon the redefinition of columns $j \rightarrow m+2-j$, we note that the matrix $\mathcal{M}_{ij} \rightarrow \mathcal{M}'_{ij} = \binom{m+j}{m+1-i}$, while the added columns are borrowed from the matrix $\mathcal{V}'_{ij} = \binom{m+1}{m+1+j-i}$, which is lower triangular with 1's on the diagonal. The matrix $\mathcal{M}(m'_1 = m+2-m_1, \dots, m'_{m+1-k} = m+2-m_{m+1-k})$ is now made of the matrix \mathcal{M}' with columns $m'_1, m'_2, \dots, m'_{m+1-k}$ erased and those of \mathcal{V}' appended. Denoting by p_1, p_2, \dots, p_k

³ We are very grateful to Saibal Mitra for this observation.

the ordered complement of the m'_i 's in $\{1, 2, \dots, m+1\}$, we may also view this matrix as made of \mathcal{V}' , with the columns p_1, \dots, p_k erased and those of \mathcal{M}' appended. Expanding the corresponding determinant with respect to these columns, we arrive at

$$\det(\mathcal{M}(m'_1, \dots, m'_{m+1-k})) = \sum_{1 \leq i_1, \dots, i_k \leq m+1} (-1)^{\sum m+1+i_r} \mathcal{M}'_{i_1, p_1} \dots \mathcal{M}'_{i_k, p_k} |\mathcal{V}'|_{i_1, \dots, i_k; p_1, \dots, p_k} \quad (2.9)$$

where the latter denotes the multiple minor of \mathcal{V}' in which lines i_1, \dots, i_k and columns p_1, \dots, p_k are erased and the determinant is taken. The latter is also equal to the determinant of single minors $\det(|\mathcal{V}'|_{i_r, p_s})_{1 \leq r, s \leq k}$, by a property satisfied by all lower triangular matrices with 1's on the diagonal. Using the multilinearity of the determinant, we write

$$\det(\mathcal{M}(m'_1, \dots, m'_{m+1-k})) = \det_{1 \leq r, s \leq k} \left(\sum_{i=1}^{m+1} (-1)^{m+1+i} \mathcal{M}'_{i, p_r} |\mathcal{V}'|_{i, p_s} \right) \quad (2.10)$$

and we finally note that

$$\sum_{i=1}^{m+1} (-1)^{m+1+i} \mathcal{M}'_{i, r} |\mathcal{V}'|_{i, s} = T_{rs}^2 \quad (2.11)$$

as a consequence of a simple binomial identity, as $|\mathcal{V}'|_{i, s} = \binom{m+s-i-1}{m}$. This completes the proof, as the sum over the m'_i amounts to that over the p_i .

So we get all the $A_{2m+2}(a, b, c, d)$ with $a + b = b + c = c + d = m + 1$ as coefficients of the polynomial $\Delta_m(\lambda)$:

$$\Delta_m(\lambda) = \det(\lambda I + T^2) = \sum_{k=0}^{m+1} \lambda^{m+1-k} A_{2m+2}(k, m+1-k, k, m+1-k) \quad (2.12)$$

with the convention that $A_n(a, 0, a, 0) = 1 = A_n(0, a, 0, a)$, as it counts the number of FPL configurations with a single set of nested arches. Moreover, according to Corollary 1, the numbers D_m are nothing but

$$D_m = \sum_{k=0}^{m+1} A_{2m+2}(k, m+1-k, k, m+1-k) = \Delta_m(1) \quad (2.13)$$

One may illustrate (2.12)-(2.13) on the first values of m

$$m = 1 : \quad T^2 = \begin{pmatrix} 2 & 3 \\ 3 & 5 \end{pmatrix} \quad \Delta_1(\lambda) = 1 + 7\lambda + \lambda^2$$

$$D_1 = 9 = 1 + A_4(1, 1, 1, 1) + 1 = 1 + 7 + 1$$

$$m = 2 : \quad T^2 = \begin{pmatrix} 3 & 6 & 10 \\ 6 & 14 & 25 \\ 10 & 25 & 46 \end{pmatrix} \quad \Delta_2(\lambda) = 1 + 63\lambda + 63\lambda^2 + \lambda^3$$

$$D_2 = 128 = 1 + A_6(2, 1, 2, 1) + A_6(1, 2, 1, 2) + 1 = 1 + 63 + 63 + 1$$

$$m = 3 : \quad T^2 = \begin{pmatrix} 4 & 10 & 20 & 35 \\ 10 & 30 & 65 & 119 \\ 20 & 65 & 146 & 273 \\ 35 & 119 & 273 & 517 \end{pmatrix} \quad \Delta_3(\lambda) = 1 + 697\lambda + 3504\lambda^2 + 697\lambda^3 + \lambda^4$$

$$D_3 = 4900 = 1 + A_8(3, 1, 3, 1) + A_8(2, 2, 2, 2) + A_8(1, 3, 1, 3) + 1 = 1 + 697 + 3504 + 697 + 1$$

etc.

Note that the above proof relies crucially on the fact that \mathcal{V}' is lower triangular with 1's on the diagonal, a property still true in general when $b = d$, while a and c are arbitrary (in which case we have $\mathcal{V}'_{ij} = \binom{a+b}{a+b+j-i}$). This leads straightforwardly to the generating function:

$$\Delta_{a+b,b+c}(\lambda) = \det_{1 \leq i, j \leq b+c} (\lambda I + U(a+b)) = \sum_{i=0}^{\min(a+b,b+c)} \lambda^{b+c-i} A_n(a+b-i, i, b+c-i, i) \quad (2.14)$$

where the matrix $U(m)$ is the m -truncated version of T^2 , namely

$$U(m)_{ij} = \sum_{r=1}^m \binom{i+r-2}{i-1} \binom{j+r-2}{j-1} \quad (2.15)$$

This gives access to all FPL numbers of the form $A_n(a, b, c, b)$ in a very compact manner.

For illustration, we have for $a+b=4$ and $b+c=6$ the following generating function

$$\begin{aligned} \Delta_{4,6}(\lambda) &= \det \begin{pmatrix} \lambda+4 & 10 & 20 & 35 & 56 & 84 \\ 10 & \lambda+30 & 65 & 119 & 196 & 300 \\ 20 & 65 & \lambda+146 & 273 & 456 & 705 \\ 35 & 119 & 273 & \lambda+517 & 871 & 1355 \\ 56 & 196 & 456 & 871 & \lambda+1476 & 2306 \\ 84 & 300 & 705 & 1355 & 2306 & \lambda+3614 \end{pmatrix} \\ &= \lambda^6 + 5787\lambda^5 + 129627\lambda^4 + 97874\lambda^3 + 1764\lambda^2 \\ &= \lambda^6 + A_{10}(3, 1, 5, 1)\lambda^5 + A_{10}(2, 2, 4, 2)\lambda^4 + A_{10}(1, 3, 3, 3)\lambda^3 + A_{10}(0, 4, 2, 4)\lambda^2 \end{aligned} \quad (2.16)$$

and the corresponding number of dimer configurations is $\Delta_{4,6}(1) = 235053$.

The determinants $\hat{D}(L, \theta)$ have occurred in different contexts [15,16,17]. In the latter of these references, the following large L asymptotic behavior is proposed:

$$\hat{D}(L, \theta) \approx A_{\text{HT}}(L)^2 \approx \left(\frac{3^3}{2^4} \right)^{L^2/4}.$$

Acknowledgements.

Many thanks to Christian Krattenthaler for his insight and his many suggestions of simplifications of the arguments of sect. 1 and of the computation of sect. 2, Saibal Mitra for a crucial observation, Rémy Mosseri for discussions, and Paul Zinn-Justin for his wonderful software, accessible on <http://ipnweb.in2p3.fr/~lptms/membres/pzinn/fpl> .

This work is partially supported by the European networks HPRN-CT-2002-00325 and HPRN-CT-1999-00161.

References

- [1] J. Propp, *The many faces of alternating-sign matrices*, preprint ([math.CO/0208125](#)).
- [2] J. de Gier, *Loops, matchings and alternating-sign matrices*, preprint([math.CO/0211285](#)).
- [3] A.V. Razumov and Yu.G. Stroganov, *Combinatorial nature of ground state vector of $O(1)$ loop model*, preprint ([math.CO/0104216](#)).
- [4] S. Mitra, B. Nienhuis, J. de Gier and M.T. Batchelor, *Exact expressions for correlations in the ground state of the dense $O(1)$ loop model*, preprint ([cond-math/0401245](#))
- [5] P. Di Francesco, P. Zinn-Justin and J.-B. Zuber, *A bijection between classes of Fully Packed Loops and plane partitions*, preprint([math.CO/0311220](#)).
- [6] F. Caselli and C. Krattenthaler, *Proof of two conjectures of Zuber on fully packed loop configurations*, preprint([math.CO/0312217](#)).
- [7] B. Wieland, *A large dihedral symmetry of the set of alternating-sign matrices*, *Electron. J. Combin.* **7** (2000) R37, ([math.CO/0006234](#)).
- [8] N.G. de Bruijn, *Algebraic theory of Penrose's non-periodic tilings of the plane*, *Kon. Neder. Akad. Wetensch. Proc. ser. A* **43** (1981) 84; *Dualization of multigrids*, *J. Phys. France, Colloques C3*, **47** (1986) C3-9.
- [9] N. Destainville, R. Mosseri and F. Bailly, *Enumeration of octagonal random tilings by the Gessel-Viennot method*, preprint([math.CO/0302105](#)).
- [10] N.C. Saldanha and C. Tomei, *An overview of domino and lozenge tilings*, *Resen. Inst. Mat. Estat. Univ. Sao Paulo* **2**, No.2, (1995) 239-252, ([math.CO/9801111](#)).
- [11] B. Lindström, *On the vector representations of induced matroids*, *Bull. London Math. Soc.* **5** (1973) 85-90;
I. M. Gessel and X. Viennot, *Binomial determinants, paths and hook formulae*, *Adv. Math.* **58** (1985) 300-321.
- [12] C. Krattenthaler, *Watermelon configurations with wall interaction: exact asymptotic results*, preprint.
- [13] P.W. Kasteleyn, *The statistics of dimers on a lattice. I : The number of dimer arrangements on a quadratic lattice*, *Physica* **27** (1961) 1209-1225; *Dimer statistics and phase transitions*, *J. Math. Phys.* **4** (1963) 287-293 ;
R. Kenyon, *An introduction to the dimer model*, preprint([math.CO/0310326](#)).
- [14] W. Jockusch, *Perfect matchings and perfect squares*, *J. Comb. Theory, Ser A* **67** (1994) 100-115.
- [15] M. Ciucu, T. Eisenköbl, C. Krattenthaler and D. Zare, *Enumeration of lozenge tilings of hexagons with a central triangular hole*, *J. Combin. Theory Ser. A* **95** (2001) 251-334;
- [16] S. Mitra and B. Nienhuis, *Osculating random walks on cylinders*, in *Discrete random walks*, DRW'03, C. Banderier and C. Krattenthaler eds, *Discrete Mathematics and Computer Science Proceedings AC* (2003) 259-264, ([math-ph/0312036](#)) .
- [17] S. Mitra and B. Nienhuis, *Exact conjectured expressions for correlations in the dense $O(1)$ loop model on cylinders* , to appear.